Suppression of Rev3, the catalytic subunit of Polζ, sensitizes drug-resistant lung tumors to chemotherapy

Jason Doles[a,b], Trudy G. Oliver[a], Eleanor R. Cameron[a], Gerald Hsu[a], Tyler Jacks[a,b,c], Graham C. Walker[b], and Michael T. Hemann[a,b,1]

[a]The Koch Institute for Integrative Cancer Research, [b]Department of Biology, and [c]The Howard Hughes Medical Institute, Massachusetts Institute of Technology, Cambridge, MA 02139

Edited by Alan R. Lehmann, University of Sussex, Brighton, United Kingdom, and accepted by the Editorial Board October 15, 2010 (received for review August 2, 2010)

Platinum-based chemotherapeutic drugs are front-line therapies for the treatment of non-small cell lung cancer. However, intrinsic drug resistance limits the clinical efficacy of these agents. Recent evidence suggests that loss of the translesion polymerase, Polζ, can sensitize tumor cell lines to cisplatin, although the relevance of these findings to the treatment of chemoresistant tumors in vivo has remained unclear. Here, we describe a tumor transplantation approach that enables the rapid introduction of defined genetic lesions into a preclinical model of lung adenocarcinoma. Using this approach, we examined the effect of impaired translesion DNA synthesis on cisplatin response in aggressive late-stage lung cancers. In the presence of reduced levels of Rev3, an essential component of Polζ, tumors exhibited pronounced sensitivity to cisplatin, leading to a significant extension in overall survival of treated recipient mice. Additionally, treated Rev3-deficient cells exhibited reduced cisplatin-induced mutation, a process that has been implicated in the induction of secondary malignancies following chemotherapy. Taken together, our data illustrate the potential of Rev3 inhibition as an adjuvant therapy for the treatment of chemoresistant malignancies, and highlight the utility of rapid transplantation methodologies for evaluating mechanisms of chemotherapeutic resistance in preclinical settings.

mouse models | error-prone synthesis | RNA interference

Cisplatin and related compounds are widely used in the treatment of a variety of malignancies. Although these agents have proven to be quite effective in treating certain tumor types, in others, such as ovarian and lung cancer, clinical success has been more variable. In particular, patients harboring advanced non-small cell lung cancer (NSCLC) generally respond poorly to aggressive chemotherapy, with median survival times commonly falling short of a year (1). In light of studies showing that nearly half of the patient population presents with advanced (stage IV) disease, it is not surprising that the 5-y survival rate for all NSCLC in the United States is less than 20%. Moreover, patients diagnosed with metastatic disease fare even worse (<4% 5-y survival) (2, 3). Therefore, a greater understanding of mechanisms of cisplatin resistance are essential to improve treatment of patients with advanced NSCLC and more broadly inform strategies to target highly drug-resistant malignancies.

Like many cytotoxic chemotherapeutic agents, cisplatin targets DNA. Although only 5 to 10% of covalently bound cisplatin is bound to DNA, it is this DNA damage that is largely responsible for its cytotoxic properties (4–6). The predominant forms of cisplatin-induced damage are intrastrand crosslinks: 1,2-(GpG) (65%), 1,2 (ApG) (25%), and 1,3 (GpNpG) (5–10%), with interstrand crosslinks and monoadducts accounting for 1 to 3% (4). Binding of HMGB proteins to 1,2-intrastrand crosslinks can contribute to cytotoxicity by shielding them from DNA repair (4, 5), although interstrand crosslinks are a particularly cytotoxic form of DNA damage (7, 8). Numerous mechanisms of cisplatin resistance have been identified, including decreasing drug uptake (e.g., by down-regulation of the copper transporter CTR1), increased efflux, and increased glutathione-based detoxification (6, 9). In addition, resistance can also arise from changes that increase a cell's capacity to either repair or tolerate DNA damage (10–12). It is this latter group of DNA repair and tolerance-based mechanisms that have come under recent scrutiny as potential contributors to clinical cisplatin resistance.

REV3L, the catalytic subunit of the DNA Polζ, which plays a key role in the DNA damage tolerance mechanism of translesion synthesis (TLS) (13, 14), is of unusual interest because of its critical role in preventing cisplatin cytotoxicity. Notably, human cells expressing reduced levels of REV3L are more sensitive to killing by cisplatin (14, 15). Additionally, in an siRNA-based screen, a reduction in REV3L sensitized human cells to killing by cisplatin to an extent equal or greater to a reduction of BRCA1 (16). Finally, chicken DT40 cells deficient in Rev3 showed the highest sensitivity to cisplatin of any of the DNA repair or checkpoint mutants tested (17). In *Saccharomyces cerevisiae*, Polζ (Rev3 and its auxiliary subunit Rev7), functions together with Rev1 in the mutagenic branch of TLS that is responsible for most mutations induced by UV light and many chemical mutagens (18). The mammalian Rev3 orthologs, human REV3L and mouse Rev3L, are nearly twice the size of *S. cerevisiae* Rev3, mostly because of one large intron (14).

In mammalian cells, as in yeast, REV1, REV3L, and REV7 are required for most of the mutagenesis induced by UV light and chemical mutagens, such as benzo(*a*)pyrene diol epoxide (19, 20). REV3L function has also been implicated in homologous recombination, somatic hypermutation, cell-cycle control, and genome stability (14, 21). Notably, in response to DNA damaging agents, such as UV light and benzo(*a*)pyrene diol epoxide, loss of Rev3 function has a greater effect on mutagenesis than cell survival (14). It seems likely that the striking sensitization to cisplatin killing caused by a reduction in REV3L levels is a result of REV3L's roles in the repair of both cisplatin-induced intra- and interstrand crosslinks (22). Consistent with this idea, inhibition of REV7 (MAD2B) or REV1, which are also involved in the repair of both intra- and interstrand crosslinks (22), similarly sensitizes mammalian cells to cisplatin (22, 23).

Little is known, however, about the effects of REV3L suppression on chemotherapeutic response in relevant preclinical settings. In this study, we examined the impact of Rev3L depletion on cisplatin response in a highly chemoresistant mouse model of late-stage lung adenocarcinoma (24). Given the striking similarities between lung tumors occurring in this Kras-driven

Author contributions: J.D., G.C.W., and M.T.H. designed research; J.D., T.G.O., E.R.C., and G.H. performed research; J.D., T.J., G.C.W., and M.T.H. analyzed data; and J.D. and M.T.H. wrote the paper.

The authors declare no conflict of interest.

This article is a PNAS Direct Submission. A.R.L. is a guest editor invited by the Editorial Board.

[1]To whom correspondence should be addressed. E-mail: hemann@mit.edu.

This article contains supporting information online at www.pnas.org/lookup/suppl/doi:10.1073/pnas.1011409107/-/DCSupplemental.

mouse model and human NSCLC, our data suggest a rationale for targeting TLS as an adjuvant therapy in the treatment of advanced lung cancer.

Results

Rev3 Deficiency Sensitizes *LSL-Kras^{G12D};p53$^{-/-}$* Lung Adenocarcinoma Cells to Cisplatin. To begin to examine the effects of Rev3L suppression on cisplatin response in a clinically relevant mouse-model system, we chose to use lung adenocarcinoma cell lines derived from previously described *LSL-Kras^{G12D};p53$^{fl/fl}$* mice. Tumors generated in this context are thought to mirror human NSCLC with respect to overt clinical phenotype, as well as to core molecular mechanisms governing adenocarcinoma development (24, 25). Interestingly, recent work has shown that autochthonous *LSL-Kras^{G12D};p53$^{-/-}$* lung tumors, like human NSCLC, also show intrinsic resistance to front-line chemotherapy (26). Most notably, these tumors proved to be refractory to cisplatin therapy, providing a system in which we could evaluate candidate drug-sensitizing genetic alterations. To this end, we designed and retrovirally expressed three unique shRNAs targeting REV3L, and subsequently verified suppression of REV3L transcript by quantitative PCR (qPCR) in virally transduced target cells (Fig. 1*A*). As impairment of TLS might have deleterious effects on cell growth or viability, we first sought to determine if our REV3L shRNAs impaired cell-cycle progression. DNA content analysis did not reveal any change in population doubling time, nor was there any cell-cycle defect, suggesting that our level of REV3L inhibition was not grossly affecting normal growth kinetics (Fig. 1 *B* and *C*). We then tested the effect of REV3L-depletion on cisplatin response and found all three shREV3L-expressing cell populations to be markedly sensitized to drug relative to vector control-infected cells (Fig. 1*D*). Additionally, when treated with a high dose of cisplatin and evaluated for long-term survival, cells lacking REV3L demonstrated a diminished capacity to recover from such an insult and conse-

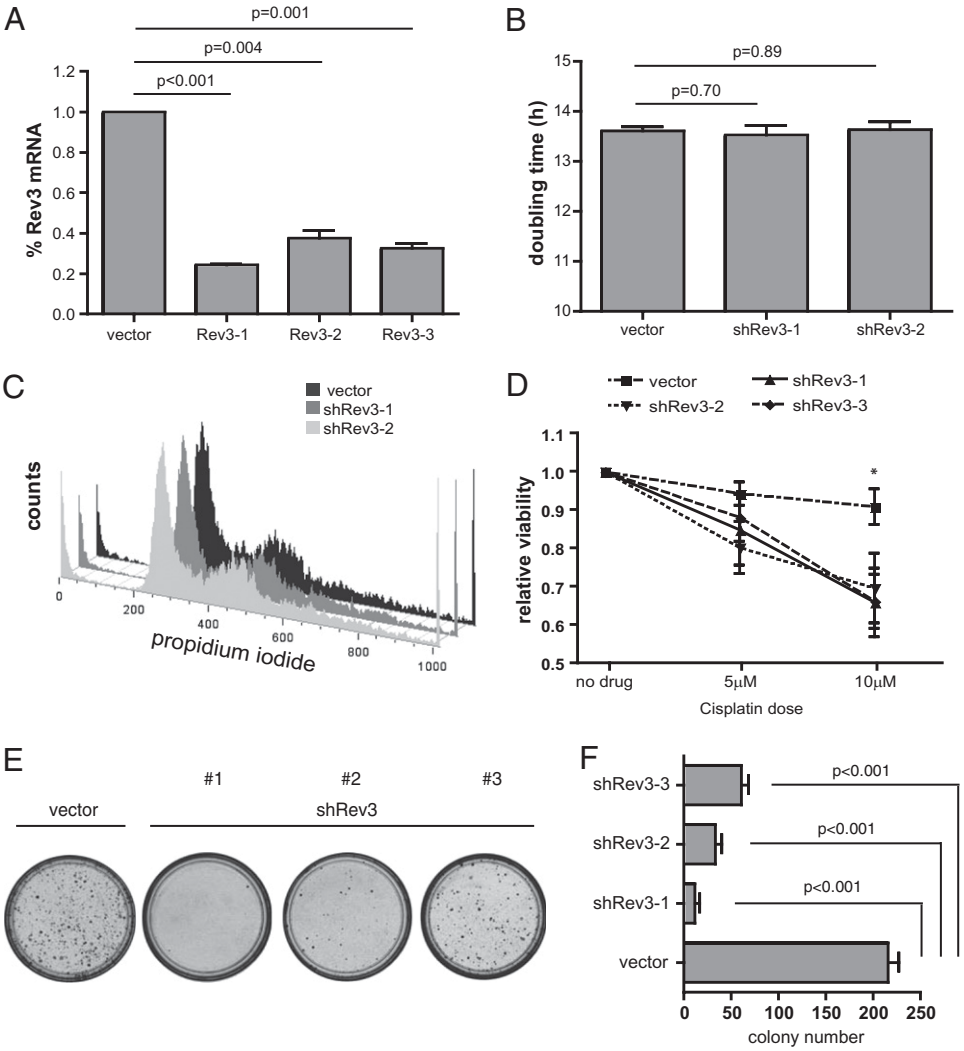

Fig. 1. Rev3-deficiency sensitizes *LSL-Kras^{G12D};p53$^{-/-}$* lung adenocarcinoma cells to cisplatin. (*A*) Quantitative RT-PCR ($n \geq 3$) confirmation of Rev3 mRNA suppression in transduced GFP sorted cell populations. Untreated control and Rev3 knock-down cells were counted and analyzed by flow cytometry to determine (*B*) overall population doubling times, and (*C*) cell-cycle distribution profiles (DNA content histogram). (*D*) Overall cell survival following cisplatin treatment was compared for adenocarcinoma cells transduced with a Rev3 shRNA or a control. Cells were then treated with cisplatin and monitored for cell survival (Cell-Titer-Glo) reagents relative to treated vector control cells ($n = 3$ independently treated samples for each construct, ± SD. $^*P < 0.05$ for all three shRev3 constructs at this dose). (*E*) A long-term (14 d) colony-outgrowth assay comparing shRev3 and vector control transduced lung adenocarcinoma cells treated with 15 μM cisplatin. The images shown depict representative 10-cm plates stained with propidium iodide to visualize colonies. (*F*) Quantification of images collected from three independently treated populations of cells. Data represent the mean colony number ± SD.

quently formed fewer colonies compared with treated control cells (Fig. 1 *E* and *F*).

REV3L deficiency in human and mouse cell lines has been associated with double-strand breaks and chromosome instability (27, 28). Consistent with these prior observations, we saw a relative increase in the number and intensity of γ-H2AX foci, a surrogate marker for DNA double-strand breaks, following cisplatin treatment of REV3L knockdown cells (Fig. 2*A*). Additionally, when examined over time by flow cytometry, REV3L-deficient cells failed to show a significant decrease in either the overall percentage of γ-H2AX–positive cells or in mean cellular γ-H2AX immunofluorescence intensity (Fig. 2*B*). Coincident with the increase in cell death associated with this enhanced level of unrepaired DNA damage, we observed a pronounced cell-cycle arrest phenotype within the surviving cell population. Specifically, cisplatin treated REV3L-deficient cells exhibited characteristics of DNA-damage induced senescence, including the appearance of a flattened, vacuolized cell morphology, as well as the induction of senescence-associated β-galactosidase activity (Fig. 2*C* and Fig. S1). Thus, REV3L suppression impairs the repair of cisplatin-induced DNA damage, leading to both cell death and irreversible cell-cycle arrest.

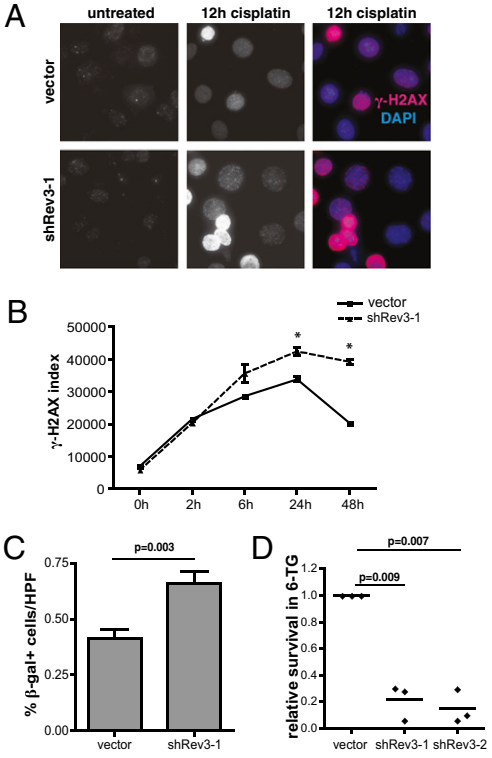

Fig. 2. Rev3 depletion promotes cisplatin-induced DNA damage but limits associated mutagenesis. (*A*) Immunofluorescence images of control and shRev3 expressing lung adenocarcinoma cells treated with 10 μM cisplatin and incubated with an anti–γ-H2AX antibody. Color images are stained with DAPI (blue) for DNA. (*B*) Flow-cytometric analysis of γ-H2AX immunofluorescence in cisplatin-treated cells. The γ-H2AX index was calculated by multiplying the number of γ-H2AX–positive cells by the mean intensity of the γ-H2AX population ($n = 3$ independently treated samples at each time point). *$P < 0.05$ at the indicated time points. (*C*) Senescent cells were identified using a standard X-gal staining protocol and manually quantified from representative microscope images. Data represent the mean of six 40× high-power fields from two independent samples for each experimental condition. (*D*) A cisplatin in vitro mutagenesis assay. Shown is the relative colony forming ability of control and Rev3-deficient cells treated with 15 μM cisplatin and then selected for 6-thioguanine resistance. Each datapoint represents an independently treated and selected experimental replicate.

Polζ is an error-prone DNA polymerase that is essential, not only for much of the mutagenesis that is caused by agents such as UV light, but for cisplatin-induced mutagenesis in human colon carcinoma cells and immortal human fibroblasts as well (15, 29). To evaluate the effect of REV3L knockdown on cisplatin-induced mutagenesis in our *LSL-Kras*^{G12D}*;p53*$^{-/-}$ cells, we performed a hypoxanthine phosphoribosyl-transferase (*hprt*) mutation assay where control and REV3L knockdown cells were treated with cisplatin, allowed to recover, and then selected in the presence of the toxic nucleoside analog 6-thioguanine (6-TG). As *hprt* function is required for 6-TG–mediated toxicity, this assay allows for the quantitation of cisplatin-induced *hprt* mutation. Cells expressing shREV3L-1 and shREV3L-2 shRNAs showed a dramatic reduction in 6-TG resistant colonies (4.7- to 6.6-fold) relative to control cells (Fig. 2*D*). Although shREV3L-3–transduced cells also showed a decrease in colony number, this decrease was not statistically significant. Notably, this shRNA also produces less cisplatin sensitization than shREV3L-1 and shREV3L-2 in colony outgrowth assays. Taken together, these cell-based assays suggest that reducing the level of REV3L not only sensitizes highly resistant lung cancer cells to cisplatin, but also prevents cisplatin-induced mutation in surviving cells.

Development of a Genetically Tractable Lung Adenocarcinoma Transplant System. Although cell-based treatment studies may yield important insight into potential tumor responses to therapy, achieving durable therapeutic responses in malignancies in their native microenvironment has proven considerably more difficult (30). Thus, we decided to evaluate the potential of REV3L inhibition as a strategy to improve upon existing cisplatin-based chemotherapeutic regimens in an established preclinical model of NSCLC. To this end, we adapted methodologies previously used for tumor transplantation in hematopoietic malignancies for use in our lung adenocarcinoma cell line (31). Such an approach allows for rapid manipulation of in vivo tumor cell genetics, without the requirement for generating stable genetically engineered mouse models. Lung adenocarcinoma cells (~5×10^4) were intravenously injected via tail vein into syngeneic immunocompetent recipient mice. As early as 20 d posttransplantation, highly proliferative tumor foci were detectable in the lung (Fig. 3*A*), with nearly every recipient mouse exhibiting a disseminated disease within 30 to 35 d (Fig. 3*B*). Notably, tumor presentation was specific to the lung, suggesting that either the route of cell delivery or the lung microenvironment restricts the development of transplanted malignancies to the appropriate target organ.

To assess the ability of these transplanted cells to recapitulate the original disease, we examined overall tumor histology. Transplanted tumors exhibited features reminiscent of their epithelial origin in the lung: namely, alveolar and sheet-like structures (Fig. 3*B*). Interestingly, we found that the transplants displayed a markedly aggressive morphology, consistent with hallmark features of late-stage carcinomas. In some cases, the transplanted tumors breached the visceral pleura, penetrating the pleural space proximal to the chest cavity (Fig. 3*B*, *Lower*, *Right*). Immunohistochemical staining of tumor specimens with antibodies targeting Nkx2.1 and HMGA2, two markers of lung adenocarcinoma progression, further suggested that these transplants represent a highly aggressive version of the disease suitable for modeling the treatment of late-stage lung cancer (Fig. 3*C*).

REV3L-Depletion Sensitizes Lung Adenocarcinoma Transplants to Cisplatin in Vivo. Using the most potent shRNA targeting REV3L, we transplanted pure populations of retrovirally infected control and REV3L knockdown lung adenocarcinoma cells into syngeneic recipient mice and allowed tumors to form (~3–4 wk). Mice were subsequently killed 48 h following cisplatin treatment

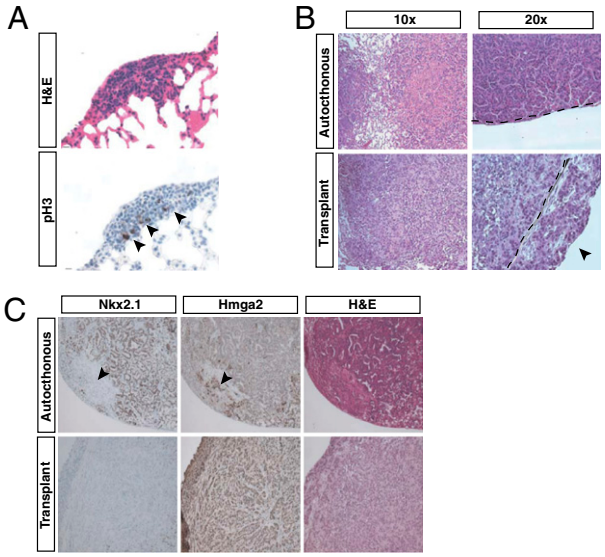

Fig. 3. Histological analysis of *LSL-Kras^{G12D};p53$^{-/-}$* adenocarcinoma transplants. (*A*) H&E (*Upper*) and antiphospho-histone-H3 (pH3) immunohistochemical (*Lower*) staining of lung adenocarcinoma transplants harvested at 18 d postinjection. Arrowheads demarcate pH3-positive cells. (*B*) H&E staining of tumor transplants harvested at 30 d postinjection, as well as representative images of an autochthonous *LSL-Kras^{G12D};p53$^{-/-}$* lung adenocarcinoma. The dotted line represents the visceral pleural boundary, with an arrowhead highlighting the tumor mass extending into the pleural space. (*C*) Anti-Nkx2.1 and anti-HMGA2 immunostaining of early- and late-stage lung adenocarcinomas, respectively. The arrowheads indicate a region in the autochthonous tumor with high expression of the late-stage marker HMGA2 and corresponding down-regulation of the early-stage marker Nkx2.1.

to analyze the effects of cisplatin on tumor-cell proliferation rate and survival. Histopathological evaluation of harvested tumors corroborated our in vitro observations, as we noted both a decrease in mitotic index (Fig. 4*A*) and an increase in apoptosis (Fig. 4*B*) in treated REV3L-deficient transplants.

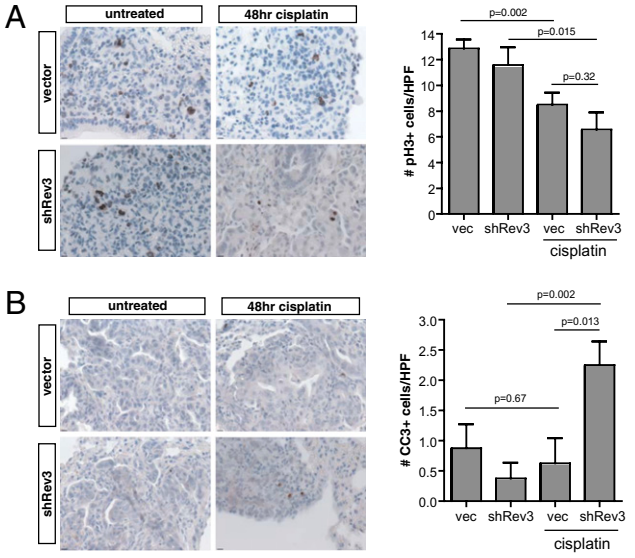

Fig. 4. Rev3 depletion sensitizes transplanted lung adenocarcinoma to cisplatin. (*A*) Anti-phosphoH3 and (*B*) cleaved caspase 3 staining of control and shRev3-transduced tumor transplants 48 h following treatment with 10 mg/kg cisplatin. Tumors were treated upon detection of tumor mass by microCT. *P* values were determined using two-tailed Student's *t* tests.

To more carefully examine the effect of REV3L suppression on lung adenocarcinoma response to cisplatin, we took an in vivo imaging-based approach that allowed us to study individual tumor dynamics over a course of therapy. Using a microcomputed tomography (microCT) imaging platform, we were able to image the lung and surrounding tissues at regular intervals to identify and subsequently track disease progression in individual tumor-bearing mice over the course of cisplatin treatment. As illustrated in reconstructed 3D isosurface and 2D axial images taken 10 d following the initiation of therapy (10 mg/kg cisplatin on day 0), Rev3-deficient transplants exhibited an enhanced response to cisplatin relative to controls (Fig. 5). This finding was evidenced at the level of individual tumors (Fig. 5 *A*–*C*), as well as in the broader context of the entire lung (Fig. 5 *D* and *E*). Indeed, quantitative evidence of overall tumor regression or at a minimum, growth stasis, was observed in cisplatin-treated REV3L-knockdown transplants, whereas most control transplants con-

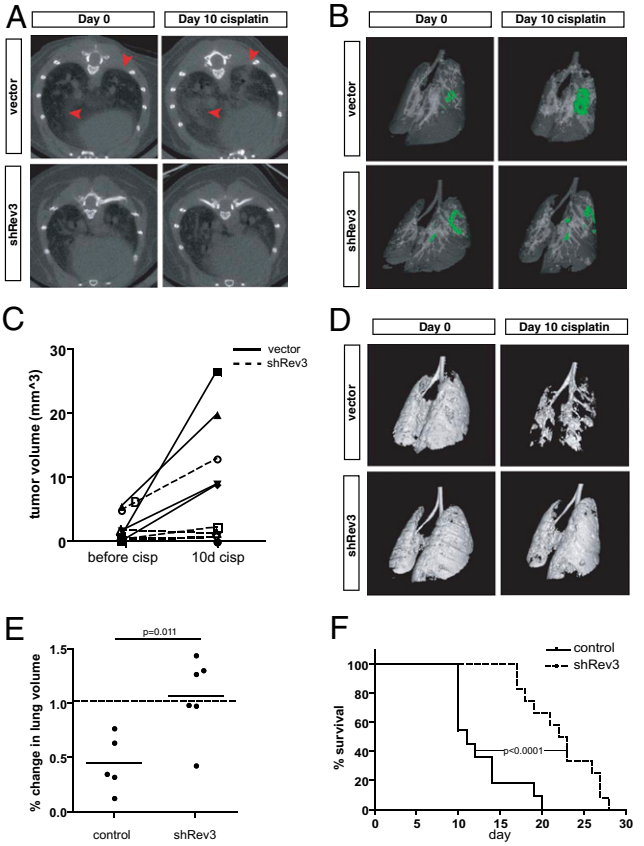

Fig. 5. Rev3 depletion promotes cisplatin efficacy in vivo. (*A*) Representative axial images of mouse lungs harboring transplanted lung adenocarcinoma cells. The darker areas represent healthy, air-filled lung space, whereas the lighter shades highlight denser tissues, including areas populated by tumor cells. Red arrowheads demarcate individual tumors in treated control mice that respond poorly to cisplatin treatment. (*B*) Three-dimensional isosurface projections of selected lung regions. Green staining indicates lung adenocarcinoma mass. (*C*) Individual tumor volume calculations for several control and shRev3 transplants. (*D*) Inverse 3D isosurface projections of healthy lung volume before and after cisplatin treatment. White/gray surfaces indicate disease-free, healthy lung space, whereas hollowed-out voids indicate the presence of tumor material. (*E*) Quantification of healthy lung volumes from *D*. *P* values were determined using a Student's *t* test. (*F*) A Kaplan-Meier curve comparing survival of mice bearing shRev3-infected transplants versus mice bearing control tumors following treatment with cisplatin (vector, $n = 11$; shRev3, $n = 12$; median survival time = 11 and 22.5 d, respectively). *P* values were determined using a log-rank test.

tinued to grow and displace healthy lung volume (Fig. 5*E*). Importantly, Kaplan-Meier analysis of overall survival supported these imaging-based observations, with mice harboring Rev3-deficient transplants surviving nearly twice as long compared with the control cohort (Fig. 5*F*).

Discussion

Our experiments provide a striking illustration of how reducing the activity of a key translesion DNA polymerase can make an intractable lung cancer model of NSCLC susceptible to cisplatin-based chemotherapy. Thus, REV3L represents a bona fide lung-cancer drug target. Inhibiting REV3L activity or expression may be particularly effective in this context, because cisplatin treatment, itself, increases REV3L mRNA levels (15) and elevated REV3L has been shown to promote cisplatin resistance (12). Notably, therapies that exploit DNA repair deficiencies, including the use of poly(ADP ribose) polymerase inhibitors in BRCA1/2-deficient tumor cells (32, 33), have emerged as a promising approach to target chemoresistant malignancies. Although it is unclear whether advanced malignancies acquire a similar dependence upon REV3L function, cell-based studies examining gliomas—a highly chemoresistant malignancy—have documented elevated levels of REV3L in this setting and shown that down-regulation of REV3L sensitizes these cells to cisplatin (12). Interestingly, mismatch repair-deficient, p53-deficient tumor cells also show increases up to 20 times in REV3L levels (34), suggesting that malignancies driven by mutagenesis in the absence of mismatch repair may be particularly reliant upon REV3L function.

The striking cisplatin sensitization seen in the absence of REV3L may result from the dual requirement for REV3L function in the repair of both intrastrand crosslinks, which constitute the majority of the lesions, and highly toxic interstrand crosslinks, which are much less frequent. The functions of Polζ (REV3L/REV7), REV1, Polη, and RAD18 are all required for replicative bypass of cisplatin intrastrand crosslink (22). Polζ has been shown to cooperate with Polη and Polκ in error-free and error-prone TLS, respectively over a 1,2-GpG cisplatin adduct (35). In addition, Polζ and REV1 have been hypothesized to facilitate repair of interstrand crosslinks independently of proliferating cell nuclear antigen monoubiquitination (22). Biochemical analyses of replication-dependent interstrand crosslink repair using *Xenopus* extracts have implicated Polζ in the TLS across from the crosslink during the repair process (36).

A potential benefit to a chemotherapeutic strategy that relies on combining a reduction in REV3L activity/expression with a DNA damaging chemotherapeutic agent is that cisplatin-induced mutagenesis might also be reduced. In vitro studies of immortal human fibroblasts have shown that reduced levels of REV3L lowers cisplatin-induced mutation, including mutation that leads to cisplatin resistance (15). In the companion article (37), we use another clinically relevant mouse model to illustrate how interfering with REV1/REV3L/REV7 pathway of mutagenic TLS can reduce the frequency of acquired drug resistance following tumor relapse.

Although specific TLS inhibitors have not yet been developed, improvements to in vivo RNAi delivery methodologies suggest that adjuvant siRNA therapies may be achievable in accessible tumor sites (38). Additionally, the development of specific inhibitors targeting critical protein interactions in TLS polymerase complexes may hold significant therapeutic promise. Although it is reasonable to believe that rapidly growing tumor cells have a greater requirement for TLS function, future work will be required to determine whether TLS inhibition can be achieved in tumors without enhancing cisplatin-related normal cell toxicity.

Genetically engineered mouse models of cancer provide the opportunity to validate candidate drug targets in relevant pathophysiologic settings (30, 39). Although autochthonous tumor models represent the ideal context for such studies, efficient mechanisms to introduce diverse genetic alterations into such models are currently lacking. This lack is particularly true for drug sensitization experiments, where all tumor cells may need to be modified to see a therapeutic effect. Here, we have developed a tumor transplant approach that allows for rapid ex vivo modification of lung adenocarcinoma cells. Importantly, transplanted tumors develop in the appropriate organ system, in the presence of an adaptive immune system, and are pathologically similar to aggressive autochthonous tumors. Although this approach does not supplant the subsequent value of autochthonous tumor models, it may inform their development. Additionally, we have recently shown that large-scale RNAi-based screening approaches can be performed in vivo (40). Thus, robust transplantation of cell lines derived from Kras-driven lung tumor models may not only serve as an attractive setting in which to evaluate putative mediators of chemotherapeutic response, but may also function as a platform from which to screen for and identify novel genetic factors capable of sensitizing aggressive NSCLC to existing chemotherapies.

Methods

Cell Culture, Retroviral Vectors, and Chemicals. Mouse lung adenocarcinoma cells were cultured in standard DMEM/10% FBS media. Short hairpin RNA constructs were designed and cloned as previously described (41). The vector used coexpressed GFP under the control of the SV40 promotor and is identical to the published MSCV/LTRmiR30-SV40-GFP (LMS) vector. Sequences (5′–3′) targeted by shRNAs are as follows: shRev3-1: TTTACTACAGATACCATGCTG; shRev3-2: TATCTTTATAAGCTGCTCCTG; shRev3-3: TACAGTTATACAAATATCCTA. Retrovirally infected cells were then selected with puromycin. Cisplatin was purchased from Calbiochem and used at the indicated concentrations (0–15 μM). For in vivo studies, cisplatin was dissolved in a 0.9% NaCl solution, protected from light, and immediately injected intraperitoneally into tumor-bearing mice. X-gal for senescent cell identification was purchased from USB Corporation.

RT-qPCR, Immunohistochemistry, and Immunofluorescence. For real-time quantitative PCR, total RNA was isolated after retroviral infection and GFP sorting for GFP-high expressing cells. RT-qPCR was performed using SYBR green on a BioRad thermal cycler. GAPDH and Rev3 primer sequences are available upon request. For immunohistochemistry assays, mice were killed by CO_2 asphyxiation and lungs were fixed overnight in 10% neutral-buffered formalin. Lung lobes were separated and embedded in paraffin according to standard procedures. Lungs were sectioned at 4 μm and stained with H&E for tumor pathology. For detection of cleaved caspase 3 (1:500; Cell Signaling) and phospho-histone-H3 (1:200; Cell Signaling), TTF-1 (Nkx2.1, 1:200; Epitomics), HMGA2 (1:500; Biocheck), tissue sections were subjected to antigen retrieval in citrate buffer, blocked in 3% H_2O_2 for 10 min, blocked for 1 h in 5% serum/PBS-T, and stained overnight at 4 °C. Secondary antibodies were used according to Vectastain ABC kits (Vector Laboratories). Cells for immunofluorescence were grown and treated on poly-L-lysine coated coverslips, fixed with 100% methanol for 5 min at −20 °C, and stored for later use. Anti–γ-H2AX (1:500; Upstate) was used along with an Alexa secondary (568) antibody (Molecular Probes) to visualize γ-H2AX foci. Stained coverslips were imaged and analyzed using Applied Precision DeltaVision instruments and deconvolution software.

In Vitro Viability Assays and FACS. For short-term viability assays, cells were seeded in triplicate (6×10^3 per well) in 96-well plates and treated as indicated with cisplatin. After 48-h treatment, cell viability was measured using CellTiter-Glo (Promega) on an Applied Biosystems microplate luminometer. Long-term viability assays were performed by initially treating 4×10^5 lung adenocarcinoma cells with 15 μM cisplatin for 24 h. Four days following treatment, cells were split 1:20 onto a fresh 10-cm plate and allowed to form colonies for ∼10 d. To visualize colonies, plates were washed with 0.05% ethidium bromide (in 50% EtOH) for 10 to 15 s and imaged using a UV-gel box/camera. Images were processed and colonies counted using ImageJ software. All flow cytometry was performed using Becton-Dickinson FACScan or MoFlo flow cytometers. Cell death was detected by propidium iodide incorporation (0.05 mg/mL), and dead cells were excluded from GFP analysis. Live cell sorting was performed using GFP coexpression as a marker of cell transduction. For γ-H2AX assays, cells were fixed in 70% EtOH, then stained using an anti-γ-H2AX antibody (1:2,500; Upstate) followed by an Alexa (488) secondary antibody. Stained cells were then costained in a sodium citrate/propidium iodide incorporation buffer before FACS analysis and subsequently analyzed using FloJo software.

Mutagenesis *(hprt)* Assay. Retrovirally transduced cells were initially cultured for a minimum of 2 wk in media containing hypoxanthine, aminopterin, and thymidine (HAT) to remove any preexisting *hprt*- variants from the population. Cells were then split into fresh media (without HAT) 24 h before treatment with cisplatin. Target cells were then mutagenized with 15 μM cisplatin for 1 h, allowed to recover, and passaged for an additional 10 d (in the absence of HAT) to stabilize any induced mutations. Mutagenized cells were then split onto fresh 10-cm plates in media containing 6-TG to select for variants with impaired *hprt* function. Resultant colonies were visualized using 0.05% ethidium bromide (see above) and imaged using a UV-gel box/camera. Images were processed and colonies counted using ImageJ software.

In Vivo Transplantation and Imaging. Lung adenocarcinoma cells ($\sim 5 \times 10^4$) were intravenously injected into the tail vein of syngeneic C57BL6/Jx129-JAE male recipient mice and monitored weekly using a GE Healthcare microCT imaging device (45-μm resolution, 80 kV, with 450-μA current) beginning 3 wk following injection. Images were acquired and processed using GE eXplore software. The Massachusetts Institute of Technology Committee on Animal Care reviewed and approved all mouse experiments described in this study.

ACKNOWLEDGMENTS. We thank members of the G.C.W. and M.T.H. laboratories for helpful advice and discussions. This study is supported in part by National Institutes of Health Grant RO1 CA128803 (to M.T.H.); Koch Institute Support (core) Grant P30-CA14051 from the National Cancer Institute; National Institute on Environmental Health Sciences Grant ES015818 and Grant P30 ES002109 from the Center of Environmental Health Sciences, Massachusetts Institute of Technology (to G.C.W.); and a Massachusetts Institute of Technology Department of Biology training grant and a Ludwig Center Graduate Fellowship (to J.D.). M.T.H. is a Rita Allen Fellow and the Latham Family Career Development Assistant Professor of Biology, T.J. is a Howard Hughes Medical Institute Investigator and a Daniel K. Ludwig Scholar, and G.C.W. is an American Cancer Society Research Professor.

1. Goss GD, et al. (2010) Randomized, double-blind trial of carboplatin and paclitaxel with either daily oral cediranib or placebo in advanced non-small-cell lung cancer: NCIC clinical trials group BR24 study. *J Clin Oncol* 28(1):49–55.
2. Finlay GA, Joseph B, Rodrigues CR, Griffith J, White AC (2002) Advanced presentation of lung cancer in Asian immigrants: A case-control study. *Chest* 122:1938–1943.
3. U.S. National Institutes of Heath National Cancer Institute (1999–2005) http://seer.cancer.gov/csr. Accessed March 2010.
4. Ahmad S (2010) Platinum-DNA interactions and subsequent cellular processes controlling sensitivity to anticancer platinum complexes. *Chem Biodivers* 7:543–566.
5. Jung Y, Lippard SJ (2007) Direct cellular responses to platinum-induced DNA damage. *Chem Rev* 107:1387–1407.
6. Fuertes MA, Castilla J, Alonso C, Pérez JM (2003) Cisplatin biochemical mechanism of action: From cytotoxicity to induction of cell death through interconnections between apoptotic and necrotic pathways. *Curr Med Chem* 10:257–266.
7. McVey M (2010) Strategies for DNA interstrand crosslink repair: Insights from worms, flies, frogs, and slime molds. *Environ Mol Mutagen* 51:646–658.
8. Schärer OD (2005) DNA interstrand crosslinks: Natural and drug-induced DNA adducts that induce unique cellular responses. *ChemBioChem* 6(1):27–32.
9. Brozovic A, Ambriović-Ristov A, Osmak M (2010) The relationship between cisplatin-induced reactive oxygen species, glutathione, and BCL-2 and resistance to cisplatin. *Crit Rev Toxicol* 40:347–359.
10. Li J, et al. (2009) Expression of MRP1, BCRP, LRP, and ERCC1 in advanced non-small-cell lung cancer: correlation with response to chemotherapy and survival. *Clin Lung Cancer* 10:414–421.
11. Larminat F, Bohr VA (1994) Role of the human ERCC-1 gene in gene-specific repair of cisplatin-induced DNA damage. *Nucleic Acids Res* 22:3005–3010.
12. Wang H, et al. (2009) REV3L confers chemoresistance to cisplatin in human gliomas: The potential of its RNAi for synergistic therapy. *Neuro-oncol* 11:790–802.
13. Friedberg E, et al. (2005) *DNA Repair and Mutagenesis* (ASM Press, Herndon, VA).
14. Gan GN, Wittschieben JP, Wittschieben BO, Wood RD (2008) DNA polymerase zeta (pol zeta) in higher eukaryotes. *Cell Res* 18(1):174–183.
15. Wu F, Lin X, Okuda T, Howell SB (2004) DNA polymerase zeta regulates cisplatin cytotoxicity, mutagenicity, and the rate of development of cisplatin resistance. *Cancer Res* 64:8029–8035.
16. Bartz SR, et al. (2006) Small interfering RNA screens reveal enhanced cisplatin cytotoxicity in tumor cells having both BRCA network and TP53 disruptions. *Mol Cell Biol* 26:9377–9386.
17. Nojima K, et al. (2005) Multiple repair pathways mediate tolerance to chemotherapeutic cross-linking agents in vertebrate cells. *Cancer Res* 65:11704–11711.
18. Waters LS, et al. (2009) Eukaryotic translesion polymerases and their roles and regulation in DNA damage tolerance. *Microbiol Mol Biol Rev* 73(1):134–154.
19. Li Z, et al. (2002) hREV3 is essential for error-prone translesion synthesis past UV or benzo[a]pyrene diol epoxide-induced DNA lesions in human fibroblasts. *Mutat Res* 510(1–2):71–80.
20. Diaz M, et al. (2003) Decreased frequency and highly aberrant spectrum of ultraviolet-induced mutations in the hprt gene of mouse fibroblasts expressing antisense RNA to DNA polymerase zeta. *Mol Cancer Res* 1:836–847.
21. Schenten D, et al. (2009) Pol zeta ablation in B cells impairs the germinal center reaction, class switch recombination, DNA break repair, and genome stability. *J Exp Med* 206:477–490.
22. Hicks JK, et al. (2010) Differential roles for DNA polymerases eta, zeta, and REV1 in lesion bypass of intrastrand versus interstrand DNA cross-links. *Mol Cell Biol* 30:1217–1230.
23. Okuda T, Lin X, Trang J, Howell SB (2005) Suppression of hREV1 expression reduces the rate at which human ovarian carcinoma cells acquire resistance to cisplatin. *Mol Pharmacol* 67:1852–1860.
24. Sweet-Cordero A, et al. (2005) An oncogenic KRAS2 expression signature identified by cross-species gene-expression analysis. *Nat Genet* 37(1):48–55.
25. Kim CF, et al. (2005) Mouse models of human non-small-cell lung cancer: Raising the bar. *Cold Spring Harb Symp Quant Biol* 70:241–250.
26. Oliver TG, et al. (2010) Chronic cisplatin treatment promotes enhanced damage repair and tumor progression in a mouse model of lung cancer. *Genes Dev* 24:837–852.
27. Brondello JM, et al. (2008) Novel evidences for a tumor suppressor role of Rev3, the catalytic subunit of Pol zeta. *Oncogene* 27:6093–6101.
28. Wittschieben JP, Reshmi SC, Gollin SM, Wood RD (2006) Loss of DNA polymerase zeta causes chromosomal instability in mammalian cells. *Cancer Res* 66(1):134–142.
29. Lin X, Okuda T, Trang J, Howell SB (2006) Human REV1 modulates the cytotoxicity and mutagenicity of cisplatin in human ovarian carcinoma cells. *Mol Pharmacol* 69:1748–1754.
30. Sharpless NE, Depinho RA (2006) The mighty mouse: Genetically engineered mouse models in cancer drug development. *Nat Rev Drug Discov* 5:741–754.
31. Burgess DJ, et al. (2008) Topoisomerase levels determine chemotherapy response in vitro and in vivo. *Proc Natl Acad Sci USA* 105:9053–9058.
32. Farmer H, et al. (2005) Targeting the DNA repair defect in BRCA mutant cells as a therapeutic strategy. *Nature* 434:917–921.
33. Bryant HE, et al. (2005) Specific killing of BRCA2-deficient tumours with inhibitors of poly(ADP-ribose) polymerase. *Nature* 434:913–917.
34. Lin X, Howell SB (2006) DNA mismatch repair and p53 function are major determinants of the rate of development of cisplatin resistance. *Mol Cancer Ther* 5:1239–1247.
35. Shachar S, et al. (2009) Two-polymerase mechanisms dictate error-free and error-prone translesion DNA synthesis in mammals. *EMBO J* 28:383–393.
36. Räschle M, et al. (2008) Mechanism of replication-coupled DNA interstrand crosslink repair. *Cell* 134:969–980.
37. Xie K, Doles J, Hemann MT, Walker GC (2010) Error-prone translesion synthesis mediates acquired chemoresistance. *Proc Natl Acad Sci USA* 107:20792–20797.
38. Wullner U, Neef I, Tur MK, Barth S (2009) Targeted delivery of short interfering RNAs—Strategies for in vivo delivery. *Recent Pat Anticancer Drug Discov* 4:1–8.
39. Van Dyke T, Jacks T (2002) Cancer modeling in the modern era: Progress and challenges. *Cell* 108(2):135–144.
40. Meacham CE, Ho EE, Dubrovsky E, Gertler FB, Hemann MT (2009) In vivo RNAi screening identifies regulators of actin dynamics as key determinants of lymphoma progression. *Nat Genet* 41:1133–1137.
41. Dickins RA, et al. (2005) Probing tumor phenotypes using stable and regulated synthetic microRNA precursors. *Nat Genet* 37:1289–1295.